TITLE: INVESTIGATING THE INFLUENCE OF SYNOPTIC-SCALE METEOROLOGY ON AIR QUALITY USING SELF-ORGANIZING MAPS AND GENERALIZED ADDITIVE MODELLING.

John L. Pearce[a*], Jason Beringer[a], Neville Nicholls[a], Rob J. Hyndman[b], Petteri Uotila[a], and Nigel J. Tapper[a]

[a] School of Geography and Environmental Science, Monash University, Melbourne, Australia

[b] Department of Econometrics and Business Statistics, Monash University, Melbourne, Australia

Keywords: air pollution, generalized additive models, self-organizing maps, and synoptic meteorology.

*Corresponding author: School of Geography and Environmental Science, Monash University, Clayton, Victoria 3800. Tel: +61399054457. E-mail: john.pearce@arts.monash.edu.au

INVESTIGATING THE INFLUENCE OF SYNOPTIC-SCALE CIRCULATION ON AIR QUALITY USING SELF-ORGANIZING MAPS AND GENERALIZED ADDITIVE MODELLING.

ABSTRACT

The influence of synoptic-scale circulations on air quality is an area of increasing interest to air quality management in regards to future climate change. This study presents an analysis where the dominant synoptic 'types' over the region of Melbourne, Australia are determined and linked to regional air quality. First, a self-organising map (SOM) is used to generate a time series of synoptic charts that classify the annual daily circulation affecting Melbourne into 20 different synoptic types. SOM results are then employed within the framework of a generalized additive model (GAM) to identify links between synoptic-scale circulations and observed changes air pollutant concentrations. The GAMs estimate shifts in pollutant concentrations under each synoptic type after controlling for long-term trends, seasonality, weekly emissions, spatial variation, and temporal persistence. Results showed the aggregate impact of synoptic circulations in the models to be quite modest as only 5.1% of the daily variance in O_3, 4.7% in PM_{10}, and 7.1% in NO_2 were explained by shifts in synoptic circulations. Further analysis of the partial residual plots identified that despite a modest response at the aggregate level, individual synoptic categories had differential effects on air pollutants. In particular, increases of up to 40% in NO_2 and PM_{10} and 30% in O_3 occur when a synoptic conditions result in a north-easterly gradient wind over the Melbourne area. Additionally, NO_2 and PM_{10} levels also showed increases of up to 40% when a strong high pressure system was centered directly over the Melbourne area. In sum, the unified approach of SOM and GAM proved to be a complementary suite of tools capable of identifying the entire range synoptic circulation patterns over a particular region and quantifying how they influence local air quality.

1. Introduction

Increased air pollutant concentrations in the urban environment do not typically result from sudden increases in emissions, but rather from meteorological conditions that impede dispersion in the atmosphere or result in increased pollutant generation (Cheng, Campbell et al. 2007). A combination of meteorological variables important to these conditions includes temperature, winds, radiation, atmospheric moisture, and mixing depth (EPA 2009). Because synoptic-scale circulations are the envelope that govern all the above meteorological features synoptic weather typing has become a popular approach for evaluating impacts of meteorological conditions on air pollution (Triantafyllou 2001; Chen, Cheng et al. 2008; Beaver and Palazoglu 2009). This has led the air quality community to recognize synoptic-scale circulations as an important driver of local air pollution (EPA 2009).

We wish to increase the understanding of the relationship between synoptic-scale circulations and air pollution in Melbourne, Australia. The city of Melbourne, with a population of approximately 3.9 million (ABS 2010), is situated on Port Phillip Bay at the south-eastern edge of continental Australia in close proximity to the Southern Ocean at 37° 48’ 49” S and 144° 57 47” E (Figure 1). The climate of Melbourne can best be described as moderate oceanic and the city is famous for its changeable weather conditions (BOM 2009). This is due in part to the city's location at the pole-ward margin of a sub-tropical continent that results in the passage of very differing air masses over the region. The mid-latitude synoptic weather systems that affect the region produce persistent westerly winds between the subtropical high pressures to the north and the Southern Ocean lows to the south. This region is also dominated by fronts, which result from the interaction of subtropical and polar air masses. Although Melbourne’s air quality can be described as relatively good when compared to other urban centres of similar size, recent periods of anomalous environmental conditions present an interesting opportunity for analysis (Murphy and Timbal 2008). During this time levels of ozone and particles have not always met air quality standards and events such as bushfires, heatwaves, and dust storms have likely influenced regional air quality. The overall objective of this research is to investigate how the dominant types of synoptic-scale circulation over Melbourne influence local air quality. Moreover, a practical methodology is presented in order to achieve these results.

2. Data

a. Large Scale Meteorological Data

The four-time daily gridded MSLP data from the ERA-Interim reanalysis (1989 to 2008) was used to develop the SOM for synoptic-scale circulations affecting Melbourne. This reanalysis was produced by the European Centre for Medium-Range Weather Forecasts (ECMWF) and is discussed in more detail by Uppala et al. (2008). MSLP fields were obtained for 10 a.m., 4 p.m., 10 p.m., and 4 a.m. local standard time (LST) for each day in the reanalysis period at a spatial resolution of 0.72° over the spatial domain of 35-44° S and 140-150° E. It is important to note that ERA40 and NCEP/NCAR reanalysis products were also trialled for this analysis. While these products produced climatologies of similar agreement ERAI was chosen as the enhanced spatial resolution of the data produced synoptic types that were more interpretable for the Melbourne region. MSLP was chosen as a proxy for atmospheric circulation because it has been shown to relate well to the spatial pattern of these processes.

b. Local Meteorological Data

Links between synoptic types and local weather conditions were made using daily automatic weather station observations for site number 086282 (Melbourne International Airport) for the period of 1999 to 2006. This site is located at 37° 40’ 12” S and 144° 49’ 48” E with an elevation of 113 m and was chosen because a comprehensive range of measures are collected on a consistent basis. Variables provided by Climate Information Services, National Climate Centre, Bureau of Meteorology Variables included:

- Maximum daily temperature (°C)
- Mean sea level pressure (hPa)
- Global radiation (MJ/m^2)
- Water vapour pressure (hPa)
- Zonal *(u)* and meridional *(v)* wind components (km/hr)
- Precipitation (mm).

Additionally, boundary layer height (BLH) was taken from the ERA-Interim data using the location of 37° 30’ 0” S and 145° 30’ 0” E for 4 p.m. LST - the approximate time of maximum boundary layer depth.

c. Air Pollutant Monitoring Data

Local air pollution data was provided by the Environmental Protection Authority Victoria (EPAV) taken from the Port Phillip Bay air monitoring network (Figure 1). Pollutants included ozone (O_3), particulate matter $\leq$ 10 µg (PM_{10}), and nitrogen dioxide (NO_2). O_3 and NO_2 concentrations are reported in parts per billion by volume (ppb) and were measured using pulsed fluorescence chemiluminescence and ultra violet absorption techniques. PM_{10} concentrations were measured using photospectrometry and are reported in micrograms per cubic meter ($\mu g/m^3$). This analysis uses the daily maximum value for 8-hr O_3, the 24-hr mean value of PM_{10}, and the daily maximum value for 1-hr NO_2 from all available monitoring locations over the period of 1999 to 2006 (Table 1). These timeframes were selected to parallel air quality objectives in the State Environment Protection Policy for ambient air quality (SEPP 1999). Additionally, days on which significant air quality events (bushfires, dust storms, factory emissions, etc.) were known to have occurred and data below 5 ppb for O_3 and NO_2 and 3 $\mu g/m^3$for PM_{10} were removed.

3. Methods

a. Self-organizing Maps

Synoptic typing is an approach used in synoptic climatology where the atmospheric state is partitioned into broad categories either in terms of the spatial patterns associated with a proxy (ex. MSLP, 500 hPa height) or the multivariate characteristics of an air mass. These synoptic categories or 'types' are then used to provide insight into the influence of large scale processes on local environmental conditions (Hewitson and Crane 2002). The classification of synoptic types used in this study was produced using a neural networking algorithm known as self-organizing maps (SOM) (Kohonen 2001). This approach was has been shown to be effective means of classifying the expected synoptic circulation patterns over a particular region (Hewitson and Crane 2002; Hope, Drosdowsky et al. 2006). In short, SOMs can be described as a data reduction technique used to visualize and interpret large high-dimensional data sets onto a two dimensional array of representative nodes (Kohonen 2001). This two dimensional array of nodes is commonly referred to as the self-organizing 'map'. One feature of the SOM that has been found particularly useful in synoptic climatology is the matching of each period in the analysis to a particular synoptic type (Hope, Drosdowsky et al. 2006). This essentially results in a time series of synoptic charts that a can be used to link environmental responses to specific types of systems through time. For more information on SOM and their application in synoptic climatology please see Hewitson and Crane (2002).

It is important to note that in practice the dimensions of the SOM are selected by the user. This has direct implications for the number of synoptic states represented. We assessed a multiple array of SOM dimensions in effort to identify a dimension that was adequate to represent the expected range of synoptic patterns for the region and practical for use in our statistical analysis. It was determined that a 4X5 array of circulation patterns met these criteria. The software used to create the SOM is part of the SOM_PAK, available from http://www.cis.hut.fi/research/som-research.

b.Generalized Additive Models

There are a multitude of techniques for analysing the effects of meteorology on air pollution (Thompson, Reynolds et al. 2001). One approach that has been found particularly effective at handling the complex non-linearity's associated with air pollution is Generalized Additive Modelling (GAM) (Aldrin and Haff 2005; Carslaw, Beevers et al. 2007). The additive model in the context of a concentration time series can be written in the form (Hastie and Tibshirani 1990):

$$g[E(y_i)] = \beta_0 + \sum_{j=1}^{n} s_j(x_{ij}) + \varepsilon_i \tag{2.1}$$

where $g[\ ]$ is a Gaussian distributed 'log-link' function, y_i is the ith air pollution concentration, $E(\ )$ is the expected concentration of y, β_0 is the overall mean of the response, $s_j(x_{ij})$ is the smooth function of ith value of covariate j, n is the total number of covariates, and ε_i is the ith residual with var(ε_i)= σ^2, which is assumed to be normally distributed. Smooth functions are developed through an integration of model selection and automatic smoothing parameter selection using penalised regression splines, which while optimizing the fit, make an effort to minimize the number of dimensions in the model (Wood 2006). Interaction terms, e.g. $s(x_1, x_2)$, can also be modelled as thin-plate regression splines or tensor product smooths. This is a notable feature for air quality applications as interaction terms have used to effectively for modelling complex responses to wind components and to account for spatial trends (Bivand et al. 2008; Carslaw 2007). The choice of the smoothing parameters is made through restricted maximum likelihood (REML) and confidence intervals are estimated using an unconditional Bayesian method (Wood 2006). This analysis was conducted using the *gam* modelling function in R environment for statistical computing (R Development Core Team 2009) with packages ‘mgcv’ (Wood 2006).

c. Model Development

The first step in the selection of individual models for O_3, PM_{10}, and NO_2 was to fit a preliminary base model. This was fit to each pollutant in order to control for the seasonality, persistence, spatial trend, and weekly emissions patterns that exist in these data. Following model (2.1) the preliminary model can be written as:

$$\log(y_i) = \beta_0 + s(time) + s(dow) + s\,(long, lat) + s\,(y_{i-1}) + \varepsilon_i \tag{2.2}$$

where *time* is a numeric vector ranging from 1 to 2922 included to account for long-term trends and seasonality, *dow* is a numeric vector ranging from 0 to 6 included to account for day-of-the-week, *long* and *lat* are the spatial coordinates of each monitor location included to account for spatial trend, and y_{i-1} is one day lag term included to account for short-term temporal persistence. It is important to note that the residual spatial variation is controlled by including a tensor product smooth , $s(long,\ lat)$, in the model and a smooth function of the preceding day’s pollutant concentration, $s(y_{i-1})$, was included to control for autocorrelation in residuals. Additionally, since air pollution data are inherently cyclic, a predetermined smoothing parameter of k=32 (one knot (k) for each change of season) was used for the construction of the spline function for *time*. The motivation for this control is that function should represent a relatively symmetric cyclic pattern in the data. To check the adequacy of our methods for controlling for space-time effects, box-plots and time-series plots of residuals by monitor location were examined. No violations of assumptions were obvious in any pollutant.

Finally, the categorical predictor for synoptic-scale circulations (C) -- included to represent synoptic-scale circulation types – was added to the model. Following model (2.1) final models can be written as:

$$\log(y_i) = \beta_0 + s(time) + s(doy) + s(dow) + s\,(long, lat) + s(y_{i-1}) + C_p + \varepsilon, \tag{2.3}$$

where the term C_p represents the effect of the pth synoptic type and $p = 0, 1, \ldots, 19$.

d. Characterization of Synoptic Influence on Air Pollution

The explanatory power of model (2.3) was measured using the R^2 statistic. The aggregate impacts of synoptic circulations on each pollutant are assessed by taking the difference in the R^2 of model (2.2) and model (2.3). Individual relationships between particular synoptic types and each air pollutant are assessed using partial response plots.

Partial response plots are used to reveal the marginal effect of each synoptic type on each air pollutant. A partial response plot shows the static effect (i.e. effects that are stable over time) of a particular synoptic type on a particular pollutant after accounting (i.e., controlling) for the effects of all other explanatory variables in the model (Camalier, Cox et al. 2007). The y-axis of each plot, which has been centred to the mean value of the response, shows the marginal effect of a covariate (Harrell 2001) on a percentage scale. Specifically, the marginal effect is the average percentage change in pollutant concentration as the covariate of interest is varied, while all other explanatory variables are kept fixed. Partial response plots make it easy to compare the size of the marginal effects of different covariates on the different pollutants.

Technically, the displayed marginal effects are given by 100 * (C_p / $C_p^{\{ref\}-1}$), where p is the synoptic type of interest, C_p is the corresponding coefficient in model (2.3), and $C_p^{\{ref\}}$ is the coefficient for the chosen reference value for p – in our case synoptic type *00*. In sum, the marginal effects are the estimated average effects of each synoptic type on the predicted values produced by model (2.3).

4. Results and Discussion

a. Self-Organizing Maps

The SOM of MSLP provides a clear visualization of the range of circulation features affecting Melbourne (Figure 2). Additionally, the method arranges the output grid so that similar types are near each other while more distinct types are further apart. Individual maps within the grid are referenced throughout the text using *XY* coordinates with category *00* being in the top left corner and category *43* being in the bottom right corner. Synoptic types with strong regions of high pressure are located near the bottom right corner of the grid while types with broad regions of low pressure are located near the top left. These pressure patterns can be used to infer regional scale wind speeds and direction along with mixing. A secondary feature of the SOM algorithm is the generation of a time series where each six hour period in the analysis has been classified under a particular synoptic type represented in Figure 2. Frequency analysis of these periodic classifications found that higher frequency nodes are presented on the periphery of the SOM grid and that lower frequency nodes are presented towards the center (Figure 3). This indicates that dominant circulations on are presented on the periphery and transitional states are presented closer to the center of the grid. It is should be noted that the transitions between synoptic features would be expected to reflect the generally eastward movement of weather systems in this region.

Meteorological conditions associated with each synoptic type were determined by matching the automatic weather station observations on any one day to the synoptic types associated with the SOM classes 10 a.m. for that day (Table 2). Across group variability for each meteorological variable indicates that each synoptic type has distinct local meteorological conditions.

b.Generalized Additive Models

b.1 Ozone (O_3)

Results found significant differences ($F=122.6$, d.f.=19, $p<.0001$) in the impact of individual synoptic-scale circulations under which marginal effects differ by up to 40% (Figure 4). Category *31*, with a frequency of 3% and an average duration of 8-hrs, was found to have the largest marginal effect on ozone concentrations at 30%. This pressure pattern, with a frequency of approximately 3.19% and an average duration of 8.28 hours, is associated with a moderate strength high-pressure system being centred over Tasmania with increased pressures extending well north of the Melbourne region and along the southern and eastern coast of Victoria (Figure 2). The pressure gradients are suggestive of a light north-easterly gradient wind over Melbourne which likely opposes the inland penetration of bay and sea breezes resulting in a blocking that impedes the dispersion of local pollutants (Tory, Cope et al. 2004). This synoptic type governed local meteorological conditions that can be characterized as having relatively high temperatures, high levels of radiation, north-easterly winds, low atmospheric moisture, and above average boundary layer height (Table 2). Similar findings on the relationship between associated local meteorology and synoptic-scale circulations that produced poor air quality were also noted in Sydney (Hart, De Dear et al. 2006). Category *03*, with a frequency of 4%, displays the largest negative marginal effect at -10%. This pattern is associated with high pressures to the north-west of Melbourne (Figure 2) and governed local conditions that can be characterized as having low temperatures and westerly winds (Table 2). The remaining circulations display some importance for ozone, but the impact for these are less pronounced. Overall, model (2.3) explained 48.7% of the variation of log transformed O_3 with the components of model (2.2) accounting for 43.6%

and the aggregate relative impact of synoptic-scale circulations accounting for a modest 5.1%.

b.2 Particulate Matter (*PM_{10}*)

Results found significant differences (F=69.42, d.f.=19, *p*<.0001) in the impact of individual synoptic-scale circulations under which the marginal effects of individual types can vary as much as 40% (Figure 5). The largest marginal effect was seen for category *21* followed closely by category *43*. Category *21*, with a frequency of 4% and an average duration of 10-hrs, displays moderately increased pressure to the east Melbourne that is likely associated with a light north-easterly gradient wind (Figure 2). Local meteorological conditions under category *21* exhibited the high temperatures, strong northerly winds, and low precipitation (Table 2). Category *43*, which occurred approximately 10% of the time with an average duration of 28-hrs, is associated with a strong high pressure system being centred directly over the Melbourne region (Figure 2). Local conditions exhibited cooler temperatures, light winds, and low boundary layer height which indicate stable conditions (Table 2). Additionally, these circulation types are characteristic of synoptic weather patterns that have high anti-cyclonicity – a factor that has been noted as important elsewhere (Leighton and Spark 1997; Triantafyllou 2001; Jacob and Winner 2009). Synoptic type *00* was found to govern periods under which particle concentrations were at their lowest in Melbourne (Figure 5). This synoptic type, with a frequency of 9% and an average duration 28-hrs, is associated with a strong low-pressure centre in the Southern Ocean with the influence of low pressure extending north of the Melbourne region. The increased pressure gradients are suggestive of an approaching cold front from the south that likely exhibits a south-westerly gradient wind which often results in a cleansing of the Melbourne air shed (Figure 2). Local conditions exhibited cool temperatures, strong westerlies, and low radiation (Table 2). All remaining circulations display some increase for PM_{10}. Overall, model (2.3) explained 41.4% of the variation of log transformed PM_{10} with the components of model (2.2) accounting for 36.7% and the aggregate relative impact of synoptic-scale circulations accounted for a modest 4.7%.

b.3 Nitrogen Dioxide (*NO_2*)

Synoptic circulation patterns were also found to be significant ($F= 133.4$, d.f.=19, $p<.0001$) for NO_2 in which the marginal effects of individual patterns varied by as much as 45% (Figure 6). The largest positive marginal effect was seen for category *31* at 40%. It is important to note that this category also resulted in the largest effect on O_3. The mechanisms under this type that are driving increases in O_3 are likely contributing to increases in NO_2. Furthermore, type *21*- the category under which the largest increases in PM_{10} occurred *also* resulted in the second highest marginal effect on NO_2. To a lesser extent increases are also seen under types *42* and *43* (Figure 6). These findings indicate that the conditions associated with increased in O_3 and PM_{10} are also associated with increased NO_2. The largest negative marginal effect for NO2 was seen for category *02* at -5%. This synoptic type, with a frequency of 5%, is associated with strong pressure gradients over the Melbourne area and is suggestive of an approaching high pressure system from the northwest. The nature of the pressure gradient suggests a south-westerly gradient wind which often results in a cleansing of the Melbourne air shed (Figure 2). Local conditions exhibited cool temperatures, strong westerlies, and low radiation (Table 2). Overall, model (3.2) explained approximately 36.7% of the variation in log transformed NO_2 over the period of 1999 to 2006 with the components of model (3.1) accounting for 29.6% of that variance. The aggregate relative impact of synoptic-scale circulations in the model was 7.1%.

c. Technical Approach

The use of the SOM technique not only supplied critical information for the development of the statistical models but also provided pertinent background information on the synoptic climatology of the region. The most beneficial aspect of using SOMs was the output provided. This included the classification of circulation features affecting Melbourne, the visualization of those features, and a time series of corresponding synoptic charts. This proved to be a robust and straightforward medium to examine the relationships between the expected range of synoptic patterns for a region and local air pollution. The challenge with using SOMs is finding the appropriate number of synoptic types. Further research is suggested to make this a more objective process.

The use of GAM clearly expanded the capabilities of this research beyond traditional studies of meteorological influences on air pollution. Historically, the majority of statistical models for air quality data have either characterized relationships based on a single monitor location or a derived univariate network summary. These approaches are limited by the inability to account for the influence of the spatial effects within a monitoring network. This is an important and often overlooked issue as networks are traditionally designed to find the maximum of a random field (Thompson, Reynolds et al. 2001). This study's approach allows the incorporation of regional-scale response information, which not only increases the statistical power of the study, but also allows us to estimate the effect of meteorological variables in isolation of network heterogeneity by including the bivariate smooth spatial trend in the model. It is important to note that Generalized Additive Mixed Models (GAMMs) were also tested in this study as they are explicitly designed to handle the grouping structure of the data. Unfortunately, this approach was not practical for the size of our data sets (Wood 2006). Additionally, comparisons between the GAM and GAMM using subsets of the data proved that our model (2.2) effectively removed the spatial effect in the data as random effects estimates were insignificant. More importantly, marginal effects estimates showed no significant changes between the two approaches.

Using a categorical predictor to represent the impact of synoptic-scale circulations on air pollutants is not without limitations. On reflection, using twenty synoptic categories served well in this particular analysis as a balance between variability and interpretability was needed, but other dimensions may have more accurately depicted the synoptic climatology of the region. Limitations of the approach are due to the measures used as controlling factors in the model, most particularly, the use of day of the week as a surrogate for emissions patterns in the region. A more precise measure of emissions would likely improve models and resulted in a more effective separation of the effect from the synoptic estimates.

5. Conclusion

These findings provide an observational foundation for diagnosing and understanding the sensitivity of O_3, PM_{10} and NO_2 in Melbourne to synoptic-scale circulations. Moreover, a complementary suite of tools capable of identifying the entire range synoptic circulation patterns over a particular region and quantifying how they influence local air quality was presented. Using this approach we identified that NO_2 was the air pollutant most responsive to changes in synoptic-scale circulations during the study period. This was followed by O_3 and then PM_{10}, respectively. Additionally, the largest increases in all pollutants were seen under synoptic types associated with north-easterly gradient wind. Notable increases were also seen for PM_{10} and NO_2 when high pressure systems were centred directly over the Melbourne region. The difference seen in air pollution under each synoptic type clearly shows that regional concentrations respond positively to high pressure systems and negatively to low pressure systems. These results provide strong evidence to the behaviour of air pollution to atmospheric circulation process and general insight into the role of local meteorology. Unfortunately, this is only part of the story for regional air quality as more pronounced responses are expected to be driven by local meteorological variables. In light of this knowledge gap, a study on focusing on how local meteorological conditions affect air pollutant concentrations in Melbourne is planned. In sum, this analysis suggests that the synoptic-scale circulations only influence regional pollutant concentrations to a moderate degree. However, the range of the effects between each synoptic type clearly identifies the important role synoptic systems have on the variability in air pollution. The unified approach of SOM and GAM proved to be a complementary suite of tools capable of identifying the entire range synoptic circulation patterns over a particular region and quantifying how they influence local air quality. This combined methodology may prove useful to air quality management in quantifying potential effect on future air quality if synoptic regimes were to change.

Acknowledgements. The authors are grateful to Sean Walsh for important contributions to this study. This study was supported through research funds provided by the Environmental Protection Authority Victoria and Monash University. Neville Nicholls involvement was supported by the Australian Research Council through Discovery Project DP0877417.

REFERENCES

ABS (2010). Regional Population Growth, Australia 2007-2008, Australian Bureau of Statistics.

Aldrin, M. and I. H. Haff (2005). "Generalized additive modelling of air pollution, traffic volume and meteorology." Atmospheric Environment **39**(11): 2145-2155.

Beaver, S. and A. Palazoglu (2009). "Influence of synoptic and mesoscale meteorology on ozone pollution potential for San Joaquin Valley of California." Atmospheric Environment **43**(10): 1779-1788.

Bivand, R. S., Edzer J. Pebesma, and Virgilio Gomez-Rubio (2008). Applied Spatial data Analysis with R. New York. Springer.

BOM. (2009). "Climate Statistics for Australian Locations." Retrieved 5 August, 2009, from http://www.bom.gov.au/climate/averages/tables/cw_086071.shtml.

Camalier, L., W. Cox, et al. (2007). "The effects of meteorology on ozone in urban areas and their use in assessing ozone trends." Atmospheric Environment **41**(33): 7127-7137.

Carslaw, D. C., S. D. Beevers, et al. (2007). "Modelling and assessing trends in traffic-related emissions using a generalized additive modelling approach." Atmospheric Environment **41**(26): 5289-5299.

Chen, Z. H., S. Y. Cheng, et al. (2008). "Relationship between atmospheric pollution processes and synoptic pressure patterns in northern China." Atmospheric Environment **42**(24): 6078-6087.

Cheng, C. S. Q., M. Campbell, et al. (2007). "A synoptic climatological approach to assess climatic impact on air quality in South-central Canada. Part I: Historical analysis." Water Air and Soil Pollution **182**(1-4): 131-148.

EPA, U. S. (2009). Assessment of the Impacts of Global Change on Regional U.S. Air Quality: A Synthesis of Climate Change Impacts on Ground-Level Ozone. U. S. E. P. Agency. Washington, DC.

Harrell, F. E. (2001). Regression modelling strategies: with applications to linear models, logistic regression, and survival analysis. New York; London, Springer.

Hart, M., R. De Dear, et al. (2006). "A synoptic climatology of tropospheric ozone episodes in Sydney, Australia." International Journal of Climatology **26**(12): 1635-1649.

Hastie, T. J. and R. J. Tibshirani (1990). Generalized Additive Models. London, Chapman & Hall.

Hewitson, B. C. and R. G. Crane (2002). “Self-organizing maps: applications to synoptic climatology.” Climate Research **22**(13-26): 14-26.

Hope, P. K., W. Drosdowsky, et al. (2006). "Shifts in the synoptic systems influencing southwest Western Australia." Climate Dynamics **26**(7-8): 751-764.

Jacob, D. J. and D. A. Winner (2009). "Effect of climate change on air quality." Atmospheric Environment **43**(1): 51-63.

Kohonen, T. (2001). Self-organizing maps, Springer.

Leighton, R. M. and E. Spark (1997). "Relationship between synoptic climatology and pollution events in Sydney." International Journal of Biometeorology **41**(2): 76-89.

Lynch, A., P. Uotila, et al. (2006). "Changes in synoptic weather patterns in the polar regions in the twentieth and twenty-first centuries, part 2: Antarctic." International Journal of Climatology **26**(9): 1181-1199.

Murphy, B. F. and B. Timbal (2008). "A review of recent climate variability and climate change in southeastern Australia." International Journal of Climatology **28**(7): 859-879.

R Development Core Team (2009). R: A language and environment for statistical computing. Vienna, Austria, R Foundation for Statistical Computing

SEPP (1999). State Environment Protection Policy (Ambient Air Quality). S19. EPA. Victoria, Australia, Victorian Government Gazette.

Spillane, K. T. (1978). "Atmospheric characteristics on high oxidant days in Melbourne." Clean Air **12**: 50-56.

Thompson, M. L., J. Reynolds, et al. (2001). "A review of statistical methods for the meteorological adjustment of tropospheric ozone." Atmospheric Environment **35**(3): 617-630.

Tory, K. J., M. E. Cope, et al. (2004). "The Australian Air Quality Forecasting System. Part III: Case study of a Melbourne 4-day photochemical smog eventt." Journal of Applied Meteorology **43**(5): 680-695.

Triantafyllou, A. G. (2001). "PM10 pollution episodes as a function of synoptic climatology in a mountainous industrial area." Environmental Pollution **112**(3): 491-500.

Uppala, S., D. Dee, et al. (2008). Towards a climate data assimilation system: Status update of ERAInterim. ECMWF Newsletter**:** 12-18.

Wood, S. (2006). Generalized Additive Models: An Introduction with R. London, Chapman and Hall.

TABLE AND FIGURE HEADINGS

Table 1. Descriptive statistics of regional air monitoring data used in model development.

Table 2. Mean values and standard deviations of observed meteorology under each synoptic type.

Figure 1. Map of meteorologic and air quality monitoring locations used in this study.

Figure 2. Synoptic types of annual MSLP pressure patterns generated using a 4X5 self-organizing map on ERAI reanalysis fields from 1989 to 2008. Individual charts represent a classified synoptic type. Reference labels are provided above of each chart.

Figure 3. Corresponding circulation pattern frequencies (%) for synoptic types identified in Figure 2. Frequencies significantly different from the expected 5% at the 95% confidence level are in boldface*.

Figures 4.The estimated marginal effect (%) along with their standard errors for each synoptic type on O_3 concentrations.

Figures 5.The estimated marginal effect (%) along with their standard errors for each synoptic type on PM_{10} concentrations.

Figures 6.The estimated marginal effect (%) along with their standard errors for each synoptic type on NO_2 concentrations.

Figure1

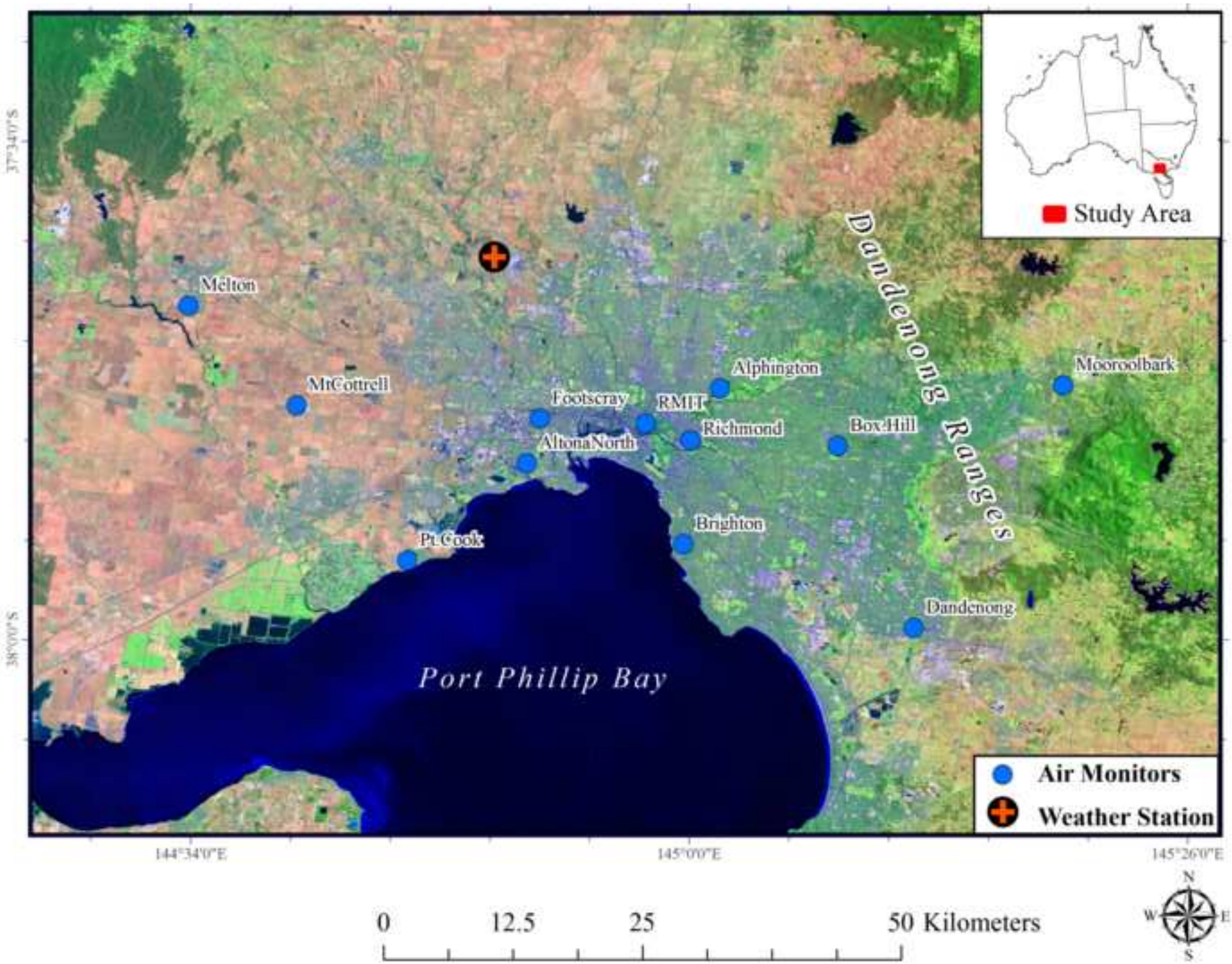

Study Area
Melton
MtCottrell
Footscray
RMIT
Alphington
Richmond
AltonaNorth
Box Hill
Mooroolbark
Dandenong Ranges
Brighton
Pt.Cook
Dandenong
Port Phillip Bay
Air Monitors
Weather Station
37°34'0"S
38°0'0"S
144°34'0"E
145°0'0"E
145°26'0"E
0
12.5
25
50 Kilometers
N
W
E
S

Figure2

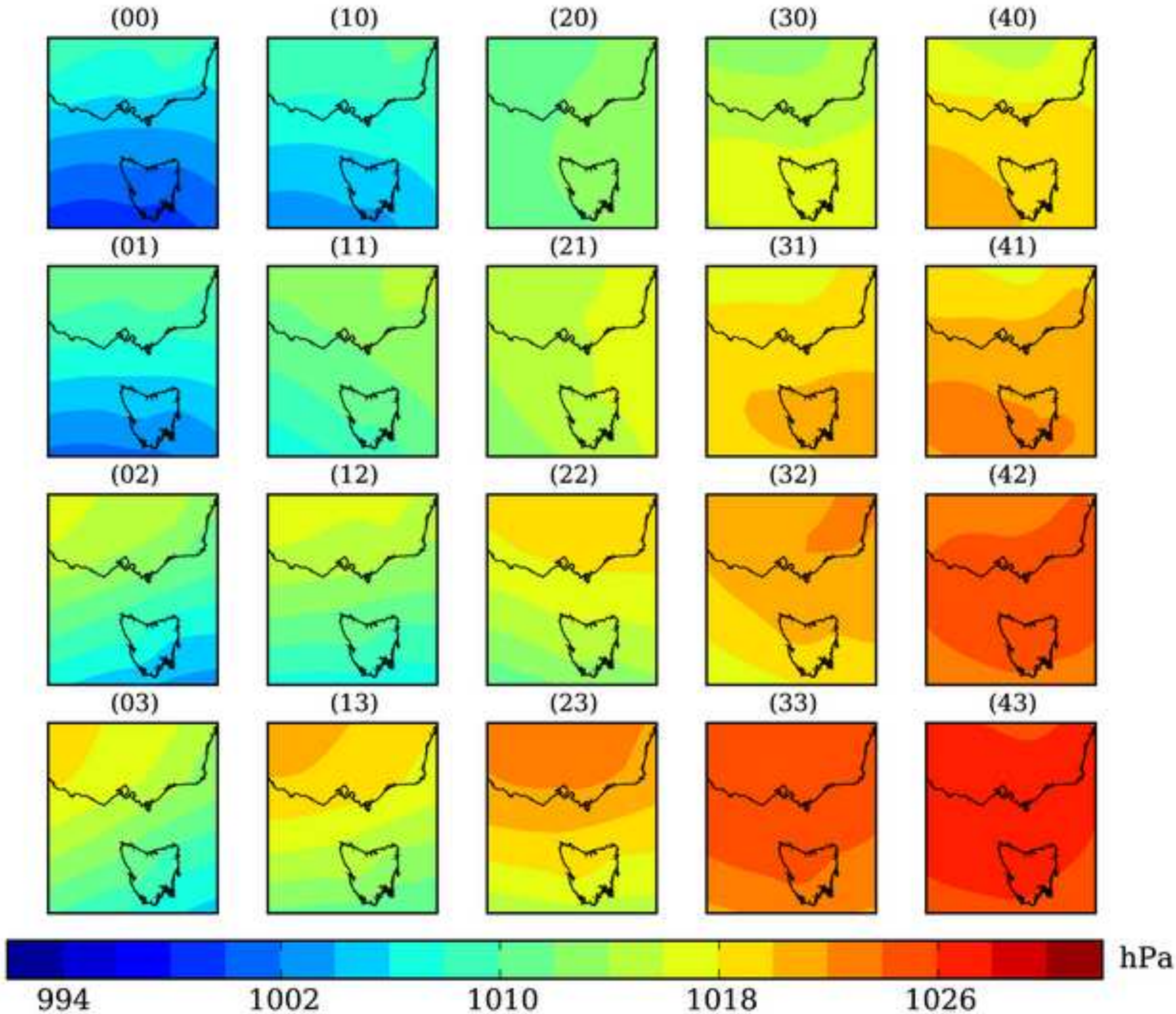
(00)
(10)
(20)
(30)
(40)
(01)
(11)
(21)
(31)
(41)
(02)
(12)
(22)
(32)
(42)
(03)
(13)
(23)
(33)
(43)
994
1002
1010
1018
1026
hPa

Figure3

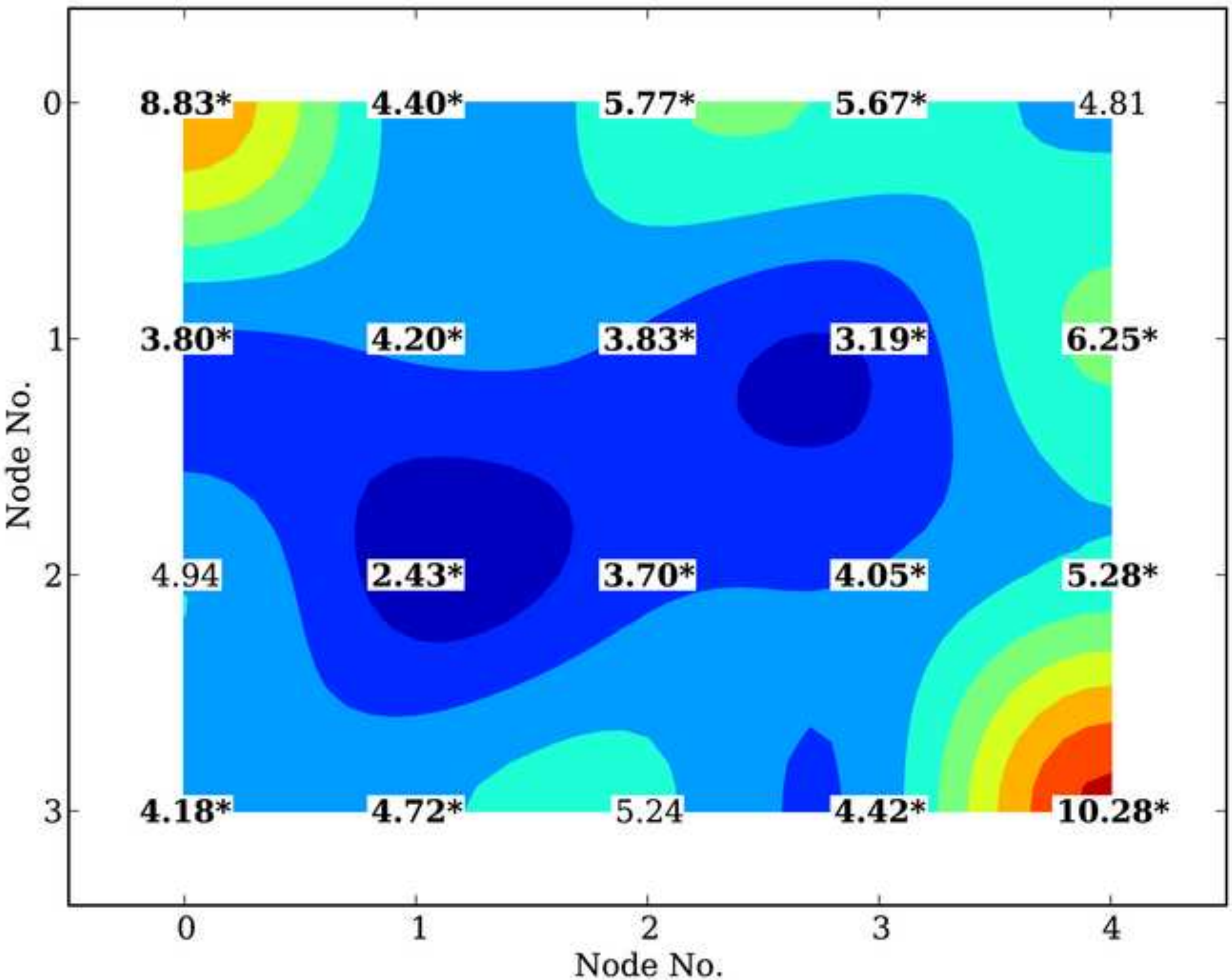
8.83*
4.40*
5.77*
5.67*
4.81
3.80*
4.20*
3.83*
3.19*
6.25*
4.94
2.43*
3.70*
4.05*
5.28*
4.18*
4.72*
5.24
4.42*
10.28*
Node No.
Node No.
0
1
2
3
4
0
1
2
3

Figure4

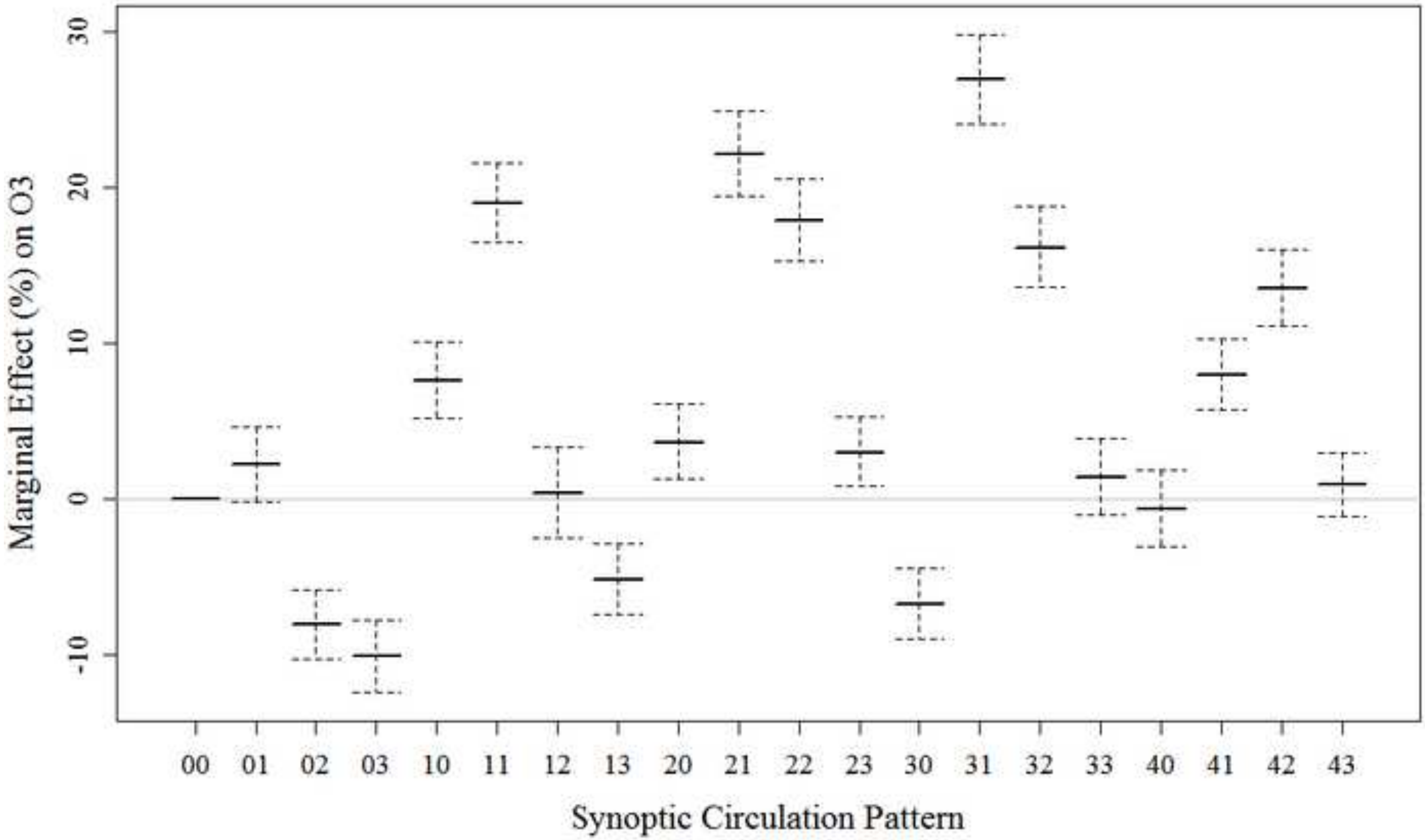

Marginal Effect (%) on O3
30
20
10
0
-10
00
01
02
03
10
11
12
13
20
21
22
23
30
31
32
33
40
41
42
43
Synoptic Circulation Pattern

Figure5

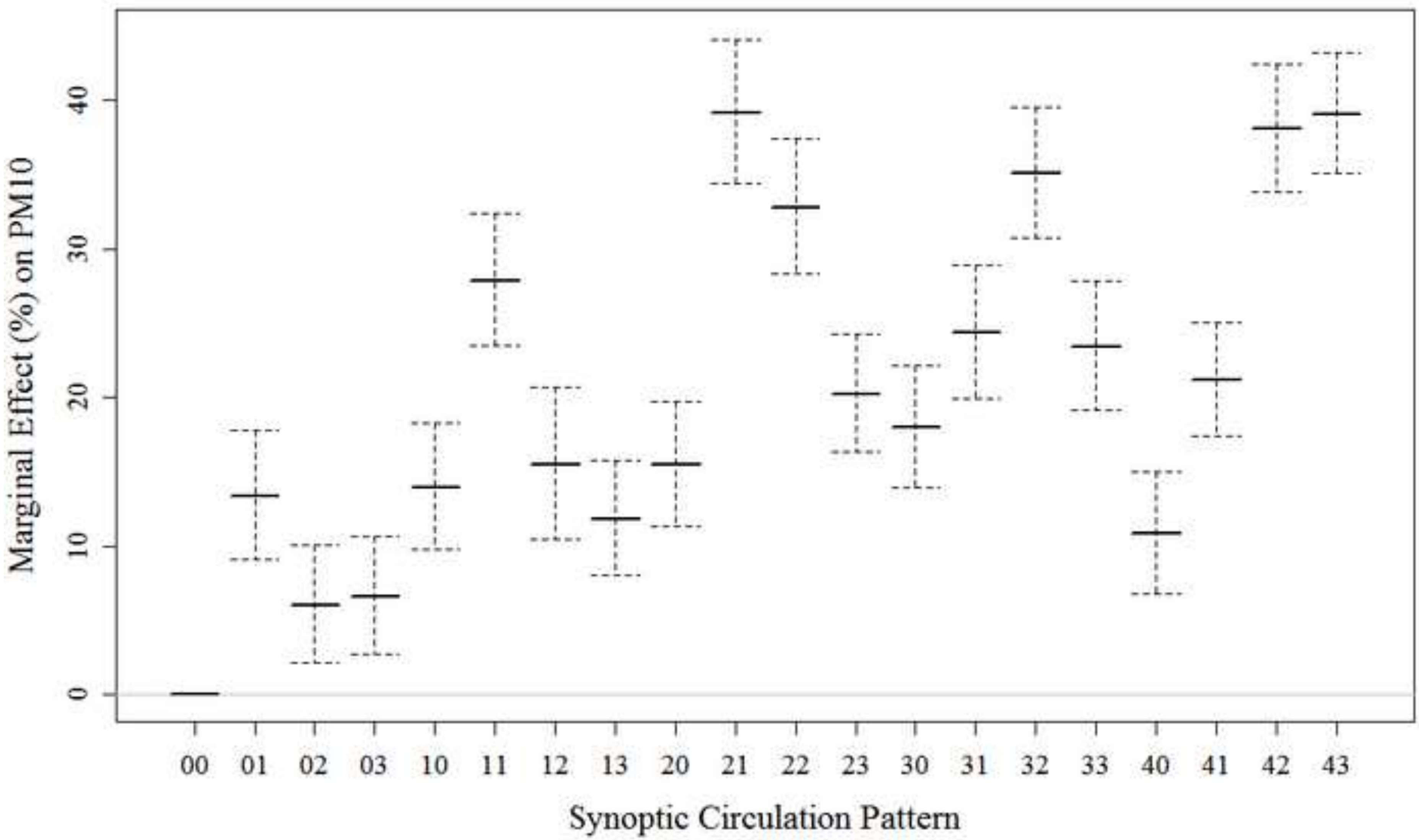
Marginal Effect (%) on PM10
0
10
20
30
40
00
01
02
03
10
11
12
13
20
21
22
23
30
31
32
33
40
41
42
43
Synoptic Circulation Pattern

Figure6

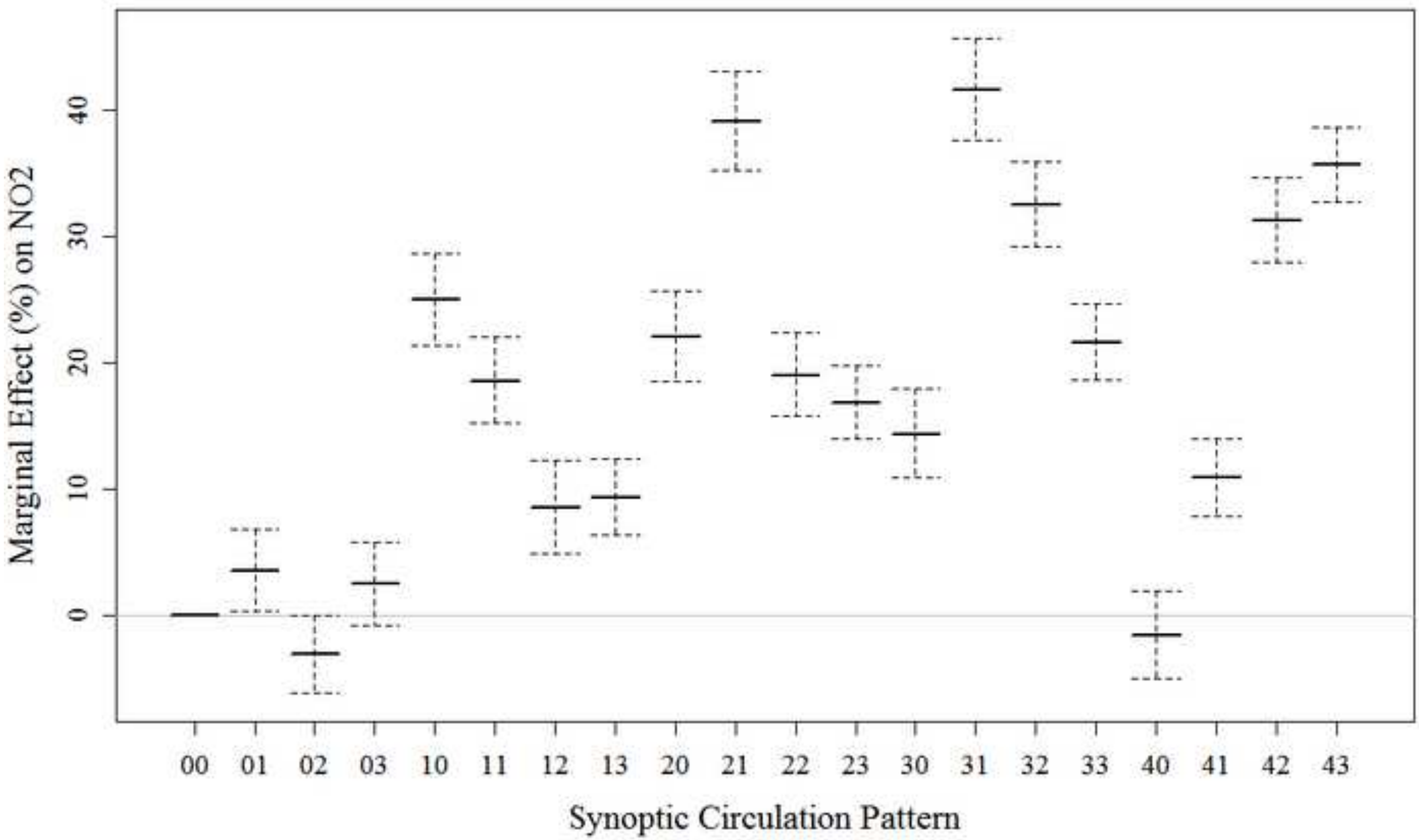

Marginal Effect (%) on NO2
0
10
20
30
40
00
01
02
03
10
11
12
13
20
21
22
23
30
31
32
33
40
41
42
43
Synoptic Circulation Pattern

Tables

Table 1. Descriptive statistics of regional air monitoring data used in model development.

	O_3 (ppb)				PM_{10} (μg/m³)				NO_2 (ppb)			
Location	Mean	SD	Min	Max	Mean	SD	Min	Max	Mean	SD	Min	Max
Alphington	20.2	8.8	5.0	63.0	17.3	6.8	3.7	76.7	23.9	8.1	5.0	69.0
AltonaNorth	21.5	9.4	5.0	87.0	--	--	0.0	0.0	23.3	10.2	5.0	79.0
BoxHill	20.7	9.3	5.0	64.0	15.2	7.4	3.6	75.3	22.0	7.7	5.0	64.0
Brighton	22.8	8.9	5.0	75.0	15.2	6.5	3.0	75.9	21.7	9.5	5.0	74.0
Dandenong	23.0	9.1	5.0	73.0	17.6	8.0	3.8	51.8	21.9	8.4	5.0	65.0
Footscray	21.7	8.2	5.0	63.0	18.0	8.0	3.6	74.5	23.6	9.7	5.0	81.0
Melton	28.1	8.7	8.0	102.0	--	--	0.0	0.0	--	--	--	--
Mooroolbark	24.5	9.0	5.0	63.0	19.3	9.2	3.2	102.8	18.1	6.6	5.0	39.0
MtCottrell	26.5	8.7	6.0	72.0	--	--	0.0	0.0	--	--	--	--
PtCook	24.2	8.6	5.0	85.0	--	--	0.0	0.0	17.1	8.9	5.0	66.0
Richmond	--	--	--	--	17.2	7.8	3.9	110.5	24.8	8.9	5.0	76.0
RMIT	16.7	7.8	5.0	61.0	18.8	7.5	4.4	82.2	26.2	9.7	5.0	90.0
Grand Total	22.2	9.2	14.0	37.0	17.1	7.7	6.6	43.2	22.5	9.3	9.0	56.0

Table 2. Mean values and standard deviations of observed meteorology under each synoptic type.

Synoptic Category	MaxTemp (°C)		WVP (hPa)		*v* wind (m/s)		*u* wind (m/s)		Rad (MJ/m^2)		Precip (mm)		MSP (hPa)		BLH (m)	
	Mean	SD	Mean	SD	Mean	SD	Mean	SD	Mean	SD	Mean	SD	Mean	SD	Mean	SD
0	18.7	5.7	10.3	2.2	13.1	12.9	-10.9	8.9	12.8	7.5	3.3	10.2	1004	3	1616	614
1	19.4	5.6	9.9	2.2	11.4	14.3	-9.5	7.9	14.1	8.1	2.2	9.1	1010	2	1673	525
2	18.4	4.3	10.2	2.2	1.0	12.9	-12.2	6.7	14.9	7.8	1.6	2.9	1013	2	1524	373
3	17.8	4.3	10.3	2.3	-6.5	9.4	-11.6	6.7	15.3	8.0	2.1	4.5	1016	2	1455	345
10	23.9	7.8	13.1	3.1	7.7	15.1	-2.9	5.3	13.9	8.9	2.6	6.1	1006	2	1722	912
11	25.6	8.5	11.6	2.7	18.8	14.5	-0.4	3.2	16.7	10.4	0.6	1.9	1011	2	1904	921
12	20.7	6.1	10.3	2.1	12.2	15.2	-4.2	3.8	15.2	8.1	0.6	1.4	1015	2	1564	554
13	17.2	3.5	10.0	1.7	-0.5	12.6	-9.0	5.8	13.7	8.1	1.0	2.3	1019	2	1297	355
20	23.6	7.2	13.8	3.5	-0.6	13.3	-1.6	5.2	17.2	10.3	3.5	10.2	1010	2	1559	840
21	27.2	7.2	11.9	2.9	15.0	11.9	0.8	3.0	19.8	9.3	0.3	1.8	1014	1	2010	857
22	21.5	6.8	9.8	2.1	22.2	14.4	0.1	3.3	14.8	8.2	0.2	0.8	1017	1	1517	680
23	17.4	4.2	9.5	1.6	6.2	15.6	-5.2	5.8	13.1	7.6	0.9	1.8	1022	2	1205	336
30	22.0	5.8	13.5	3.2	-7.7	9.1	-2.6	4.6	17.6	9.9	1.7	4.6	1014	2	1381	643
31	25.9	6.8	12.3	2.8	4.0	12.0	0.4	3.3	22.0	8.9	0.3	1.4	1017	1	1848	759
32	21.2	6.2	10.3	2.2	12.4	14.8	0.0	3.2	16.2	9.1	0.6	2.4	1020	2	1370	645
33	15.9	3.2	9.3	1.5	5.1	13.6	-4.3	5.5	10.8	5.8	0.7	2.1	1026	2	1050	306
40	20.1	4.8	12.5	2.6	-13.6	7.8	-2.9	4.5	17.6	9.9	2.5	6.1	1017	2	1326	425
41	22.1	5.3	12.2	2.4	-10.0	9.8	-1.7	4.5	20.1	9.2	1.3	4.3	1019	2	1556	559
42	20.9	6.1	10.7	2.2	-1.7	12.4	-0.7	4.0	18.3	9.3	0.8	3.1	1022	1	1415	584
43	17.0	4.3	9.8	1.7	0.5	10.9	-1.9	3.7	12.3	6.8	0.4	1.2	1028	3	1064	401